Astron. Astrophys. 345, 276–281 (1999)

ASTRONOMY AND ASTROPHYSICS

Mean free path and energy loss of electrons in the solar corona and the inner heliosphere

C. Estel and G. Mann

Astrophysikalisches Institut Potsdam, An der Sternwarte 16, D-14482 Potsdam, Germany

Received 11 December 1998 / Accepted 4 February 1999

Abstract. We have studied the mean free path of electrons in the solar atmosphere in dependence on their initial velocity and their starting height above the photosphere. The net pitch angle change results from the combined effects of Coulomb scattering and the decreasing field strength of the large-scale magnetic field. We show that above a certain velocity all electrons can travel a distance of at least five AU without deflection. This treshold velocity decreases with increasing starting height. Furthermore the loss of kinetic energy due to Coulomb collisions as a function of distance from the Sun has been calculated. At small distances, up to at least 1.5 $R_\odot$ (solar radius), the energy component parallel to the magnetic field (assumed as radial from the Sun) decreases but above 1.5 $R_\odot$ this component increases though the total particle energy decreases. If we assume that the injected electrons also have a velocity component perpendicular to the magnetic field (pitch angle $\theta > 0$), the radial velocity component will increase even at low coronal heights. The theoretical results are compared with observational data of solar type III radio bursts.

Key words: plasmas – Sun: corona – Sun: flares – Sun: radio radiation

1. Introduction

Electrons accelerated in a solar flare to high energies (0.1c - 0.5c) produce electromagnetic emissions of various kinds (X-ray, microwave- and radio bursts) (see Benz 1993 as a review) and are accessible in direct particle detection experiments (e.g. Lin et al. 1996). One convincing way to follow an electron beam propagating outwards from the Sun provide observations in the radio frequency range. Electron beams which travel through the coronal and interplanetary plasma can generate Langmuir waves via a beam-plasma instability with a frequency of about $f_P = (n_e e^2/\pi m_e)^{1/2}$. A part of the energy of the Langmuir waves is converted into electromagnetic radiation with frequencies near the fundamental of the local plasma frequency, f_P, or its harmonic $2f_P$, or both. This occurs due to coalescence of Langmuir waves with low frequency waves at f_P. The harmonic radiation is generated by coalescence of two Langmuir waves (Melrose 1985). These processes produce a characteristic radiation signature in the radio frequency range - the type III bursts. Within the classification of type III bursts, there exist several sub-categories (see Suzuki & Dulk 1985, Bastian et al. 1998). There are isolated bursts which can travel up to 1 AU or even more and produce interplanetary radio bursts. On the other hand we observe high-frequency bursts whose low frequency cutoff (about 150 MHz) is still visible in ground based observations, i.e. the associated electron beams cannot escape from low coronal heights.

The variety of type III bursts shows that the propagation of electron beams is influenced by various interaction processes with the charged particles of the coronal and interplanetary plasma (e.g. Coulomb collisions, effects of the nonuniform interplanetary magnetic field, wave-particle interactions of numerous kinds) (see Karlický 1997 as review). Because of the wide range of possible plasma parameters a systematic study of the electron propagation process is necessary. The mean deflection angle and mean energy loss due to Coulomb collisions were analytically studied by Brown (1972) for electrons that are accelerated downward into the dense chromosphere and by Emslie (1978) under more general conditions. Bai (1982) included the effects of an inhomogeneous magnetic field and applied the model to electrons that travel in a coronal loop geometry. The time independent Fokker-Planck equation for electrons undergoing Coulomb collisions in a magnetized plasma was numerically solved by Leach & Petrosian (1981). Analytic solutions of the time-dependent Fokker-Planck equation for electrons in a homogeneous magnetized plasma are given in Lu & Petrosian (1988).

By means of the analytical expressions for the mean deflection angle we have calculated the mean free path of electrons which propagate outwards from the Sun under the influence of Coulomb collisions and the decreasing field strength of the large scale interplanetary magnetic field. Solar flares do not only occur at the photospheric or low coronal levels but also at higher coronal heights (up to half a solar radius). Besides solar flares electrons can be accelerated at a shock wave at even higher altitudes. Therefore we have studied the mean free path as a function of starting height in the solar corona and the initial velocity of the electrons. Furthermore we have calculated the

Send offprint requests to: C. Estel

kinetic energy loss as a function of distance from the Sun and as a function of initial velocity and initial pitch angle.

In Sect. 2 of this paper we present the analytic expressions for the mean scattering angle and energy loss due to Coulomb collisions and for the pitch angle change in an inhomogeneous magnetic medium. The resulting path lengths are given in Sect. 3.1. In the last chapter (Sect. 3.2) we discuss the kinetic energy loss as a function of radial distance from the Sun.

2. The model

2.1. Coulomb collisions

An electron that travels through a fully ionized hydrogen plasma is deflected from its original propagation direction due to Coulomb collisions. The mean square scattering angle for an electron that passes a distance Δx is given by (small-angle approximation) (e.g. Jackson 1962):

$$\langle(\Delta\theta_C)^2\rangle = 2\frac{\mathrm{e}^4}{2\pi\varepsilon^2\mathrm{m_e^2}}\ln(\Lambda)\int\frac{\mathrm{n(x)}}{\mathrm{v(x)}^4}\mathrm{dx} \tag{1}$$

with:

$$\Lambda = \frac{\mathrm{b_{max}}}{\mathrm{b_{min}}} = 4\pi\varepsilon\frac{\lambda_\mathrm{D}\mathrm{m_e v_0^2}}{\mathrm{e^2}} \tag{2}$$

(b: impact parameter, λ_D: Debye length). With the densities and velocities considered in this work $\ln(\Lambda)$ has values between 20 and 35.

With the approximation for small-angle deflections ($\tan(\theta/2) \approx \theta/2$) the center of mass (c.m.) scattering angle is given by:

$$\frac{\theta}{2} = \frac{1}{4\pi\varepsilon}\frac{\mathrm{e}^2}{\mu\mathrm{v_0^2 b}} \tag{3}$$

with $\mu = \mathrm{m_1 m_2/(m_1+m_2)}$ is the reduced mass. For electron-proton collisions: $\theta_\mathrm{lab} = \theta$ and $\mu = \mathrm{m_e}$; for electron-electron collisions: $\theta_\mathrm{lab} = \theta/2$ and $\mu = \mathrm{m_e}/2$. Thus, electron-electron collisions and electron-proton collisions contribute the same amount to the net deflection angle in the laboratory system. This gives the factor 2 in Eq. (1). If the mass of the fast particle is higher than or approximately equal to the mass of the thermal particles in the plasma the fast particle will loose kinetic energy. For e-e collisions the kinetic energy loss is given by (with $\Delta\mathrm{v} \ll \mathrm{v}$) (Trubnikov 1965):

$$\mathrm{dE} = \frac{\mathrm{n(x)e^4}}{4\pi\mathrm{m_e}\varepsilon^2}\frac{\ln(\Lambda)}{\mathrm{v(x)}^2}\mathrm{dx}, \tag{4}$$

The deceleration of electrons is (with E=mv^2/2):

$$\mathrm{dv} = \frac{\mathrm{n(x)e^4}}{4\pi(\mathrm{m_e}\varepsilon)^2}\frac{\ln(\Lambda)}{\mathrm{v(x)}^3}\mathrm{dx}, \tag{5}$$

for e-p collisions dv/dx is $\mathrm{m_e/m_p}$ times less than in the case of e-e collisions.

2.2. Nonuniform magnetic field

An electron that starts in the solar corona and travels into the interplanetary space follows the interplanetary extension of the solar magnetic field. Provided that the spatial variations of the magnetic field are small ($|\mathrm{v}\nabla B/\omega_\mathrm{c}B| \ll 1$), the magnetic moment $\mu = \mathrm{W_\perp/B}$ will be an approximate constant of the motion (see Krall & Trivelpiece 1973). The magnetic field strength decreases with increasing distance from the Sun. Thus, the velocity component perpendicular to the magnetic field and the pitch angle (angle between magnetic field and particle velocity) decrease as well. From the conservation of the magnetic moment follows:

$$\sin(\theta)\sqrt{\frac{B_2}{B_1}} = \sin(\theta + \Delta\theta_B). \tag{6}$$

$\mathrm{B_1}$ and $\mathrm{B_2}$ are the magnetic field strengths at the two path ends of the path Δr, $\Delta\theta_B$ is the change of the pitch angle after passing the path Δr and θ is the pitch angle. With the assumptions $\Delta\theta_B \ll 1$ and $|(\mathrm{B_2}\text{-}\mathrm{B_1})/\mathrm{B_1}| \ll 1$ the pitch angle change due to the gradient of the magnetic field is:

$$(\Delta\theta)_\mathrm{B} = \frac{1}{2}\tan(\theta)\left(\frac{\mathrm{B_2}}{\mathrm{B_1}} - 1\right). \tag{7}$$

In Bai (1982) it was shown that the total pitch angle change after passing a path Δr is given by:

$$\Delta\theta = (\Delta\theta)_\mathrm{C} + (\Delta\theta)_\mathrm{B}, \tag{8}$$

on the condition that Δr is taken such that $(\Delta\theta)_\mathrm{C} \ll 1$ and $(\Delta\theta)_\mathrm{B} \ll 1$.

The total path of the particle Δx can be expressed by the radial distance Δr and the pitch angle ($\mathrm{v_r}$ is the radial velocity):

$$\cos(\theta) = \frac{\Delta\mathrm{r}}{\Delta\mathrm{x}} = \frac{\mathrm{v_r}}{\mathrm{v}}. \tag{9}$$

2.3. Density model and magnetic field model

In the present work we have used a density model by Mann et al. (1999) who have numerically solved the spherical symmetric magnetohydrostatic equations (see Fig. 1). A heliospheric density model was obtained as a special solution of Parkers's wind equation by taking a temperature of one million degrees and the long duration averages of the particle number density and the particle flux at 1 AU based on observations of the Helios 1 and 2 and the IMP satellites (Schwenn 1990). The model covers a range from 1.01 $\mathrm{R_\odot}$ up to 5 AU and agrees very well with different density measurements.

To describe the change of the magnetic field between 1.02 $\mathrm{R_\odot}$ and 10 $\mathrm{R_\odot}$ we have used the empirical model by Dulk & McLean (1978):

$$\mathrm{B} = 0.00005\left(\frac{\mathrm{r}}{\mathrm{R_\odot}} - 1\right)^{-\frac{3}{2}} \qquad [\mathrm{Tesla}]. \tag{10}$$

Above 10 $\mathrm{R_\odot}$ the radial component decreases with (Mariani & Neubauer 1990):

$$\mathrm{B_r} = \mathit{const1}\,\frac{1}{\mathrm{r^2}} \tag{11}$$

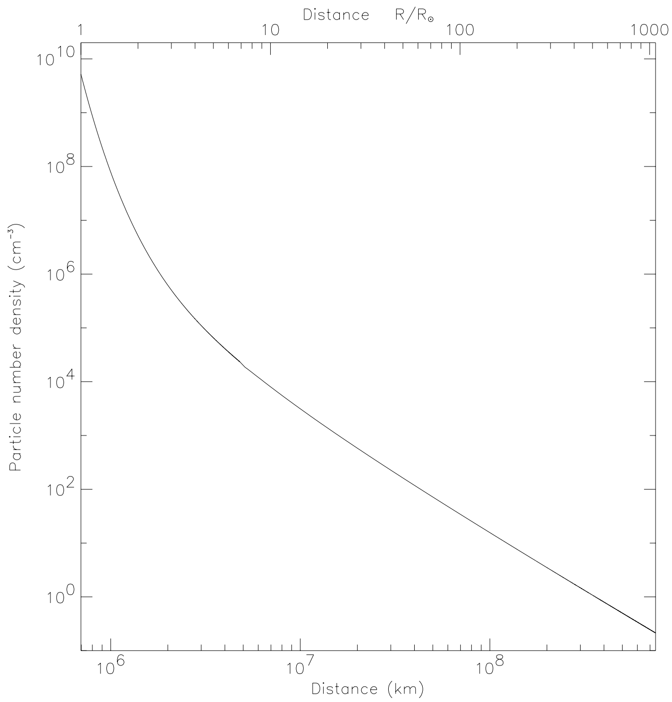

Fig. 1. Radial distance of the particle number density (after Mann et al. 1999).

and the azimuthal component with

$$B_\varphi = const2 \frac{1}{r^{1.1}}. \tag{12}$$

Const1=8.969x10^{13} Tm^2 has been deduced from the magnetic field strength at 10 $R_\odot$ (given by the model by Dulk and McLean) and *const2*=9806.69 $Tm^{1.1}$ from B_φ(1AU)=5nT (Mariani & Neubauer 1990). This gives a total magnetic field strength of B=$\sqrt{B_r{}^2 + B_\varphi^2}$=6.4nT at a distance of 1 AU.

3. Results and discussion

3.1. Mean free path

We have studied the propagation of electrons as a function of initial velocity and starting height in the solar corona. The mean free path or stopping height results from that distance where the pitch angle has a value of π/4, since above this value the particles are not any longer a system with a narrow angular distribution in the sense of a beam. The results for a starting height of 1.05 $R_\odot$ (all distance values in this paper refer to the center of the Sun) are summarized in Table 1 (upper part). The third column contains the final velocity of the particle at the stopping height which is given in column two. The last two columns contain the final pitch angle due to Coulomb collisions and the total pitch angle, respectively.

As a result we have found that electrons with initial velocities below 65 000 km/s stop at a distance below 1.5 $R_\odot$ already but electrons with velocities above this value can reach a distance of 5 AU (calculation range) without any deflection and without a considerable loss of kinetic energy.

Table 1. Mean free path (R/$R_\odot$), final velocity (v_{final}), Coulomb scattering angle ($\Delta\theta_c$) and deflection angle ($\Delta\theta$) if both Coulomb collisions and effects of the large-scale interplanetary magnetic field are considered as a function of initial velocity (first column) for a starting height of 1.05 $R_\odot$. The results of the upper part were obtained with the density model by Mann et al. (1999) (1075 $R_\odot \hat{=}$ 5 AU corresponds to the calculation range). The lower part represents the results obtained with four times the Newkirk model (10 $R_\odot$: validity range of the model).

v_o (10^4 km/s)	R/$R_\odot$	v_{final} (10^4 km/s)	$\Delta\theta_c$	$\Delta\theta$
Density model of Mann et al. (1999)				
2.0	1.05	1.71	45.2	45.0
3.0	1.05	2.55	46.9	45.0
4.0	1.06	3.34	48.3	45.0
5.0	1.07	3.99	54.4	45.1
6.0	1.15	4.08	71.1	45.0
6.5	1075	3.74	85.1	0.1
7.0	1075	5.44	57.4	0.1
8.0	1075	7.15	38.3	0
9.0	1075	8.45	28.7	0
10.0	1075	9.61	22.7	0
4·Newkirk model				
2.0	1.05	1.71	45.3	45.1
3.0	1.05	2.54	46.3	45.1
4.0	1.06	3.32	49.2	45.0
5.0	1.08	3.92	56.3	45.0
6.0	1.16	4.03	72.1	45.0
6.5	1.37	3.46	90.8	45.0
7.0	10	4.56	74.9	5.5

The lower part of Table 1 shows the results obtained with four times the Newkirk model (Newkirk 1961):

$$N = \alpha N_0 10^{4.32 \frac{R_\odot}{r}} \tag{13}$$

with α=4 and N_0=4.2x$10^{10}m^{-3}$. Due to the higher densities at distances above 1.11 $R_\odot$ compared to the model of Mann et al. (1999) the threshold velocity slightly shifts to higher values (65 000 km/s).

The influence of different starting heights is depicted in Fig. 2. The starting height is given by the intersections between the curves and the distance axis. The frequency values written on the second ordinate correspond to the plasma frequency calculated by means of the density model by Mann et al. (1999). With increasing starting height the threshold velocity, above which the mean free path becomes nearly infinity, shifts to lower values.

3.2. Kinetic energy loss

In Fig. 3 the total velocity (right) and the radial velocity component (parallel to the magnetic field) (left) are shown as a function of distance from the Sun. The total velocity has been calculated by means of Eq. (5). The radial velocity component at a given

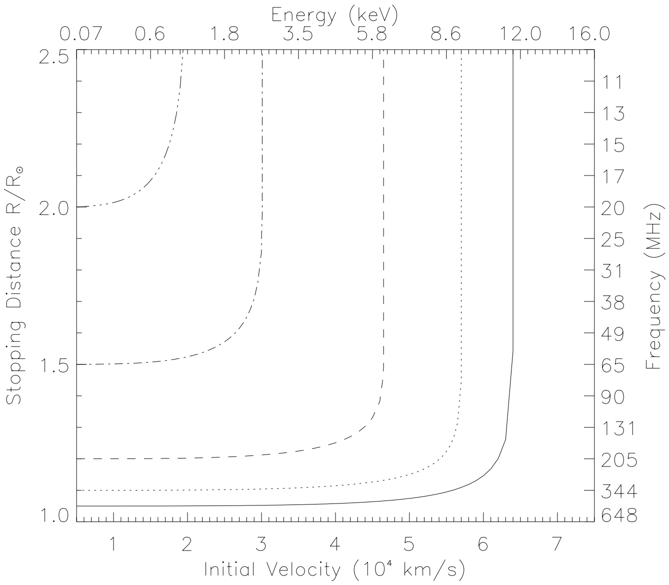

Fig. 2. Stopping distance as a function of initial velocity for different starting heights in the solar corona. The starting height is given by the intersection between the curves and the distance axis, i.e. 1.05 $R_{\odot}$, 1.1 $R_{\odot}$, 1.2 $R_{\odot}$, 1.5 $R_{\odot}$ and 2.0 $R_{\odot}$. All distances are related to the center of the Sun.

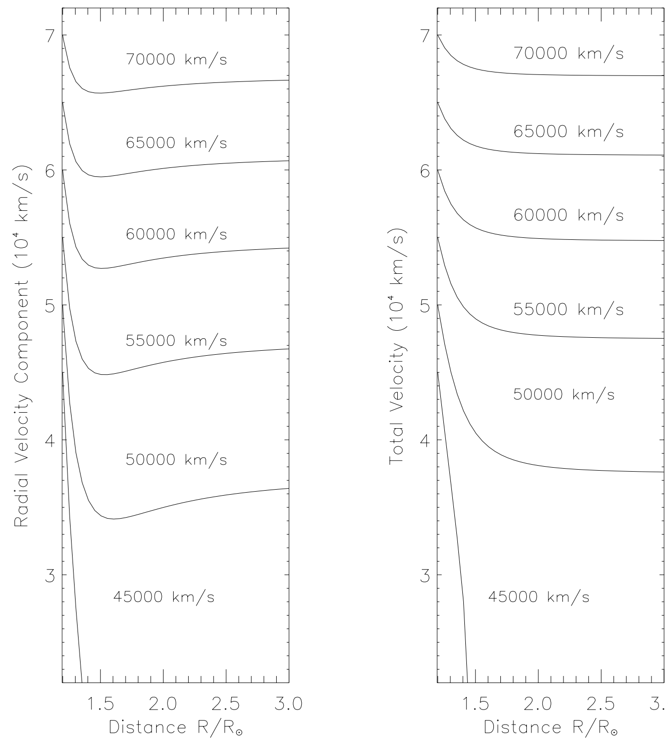

Fig. 3. Total velocity (*right*) and radial velocity component (*left*) as a function of distance from the Sun for several initial velocities. The starting height was 1.2 $R_{\odot}$.

position has been derived from the simple trigonometrical equation: $v_r = v\cos(\theta)$.

Electrons are decelerated due to Coulomb collisions with the thermal electrons of the ambient plasma. Therefore the total velocity component decreases with increasing altitude. A considerable part of the kinetic energy is deposited at altitudes below 2 $R_{\odot}$. Against this the radial velocity component decreases at small distances only, but at about 1.5 $R_{\odot}$ it starts to increase. The cause is that at greater distances the influence of the magnetic field exceeds the angular deflection due to Coulomb collisions. At higher altitudes, where the pitch angle is equal to zero $(\theta = 0)$, the radial velocity component becomes equal to the total velocity of the particle.

Lin et al. (1996) considered the energy loss for one special electron event. Because of the low energy of the detected electrons near 1 AU (down to 0.5 keV) they concluded, that the particles must have been accelerated high above the photosphere (about 2 $R_{\odot}$ from the center of the Sun). This is in very good agreement with our results (Fig. 2).

Dulk et al. (1987) have studied the radial velocity dependence of electrons by examination of a set of 28 interplanetary type III bursts. They found no evidence for a systematic increase or decrease of exciting electron speed in their data. 21% of the bursts indicated increasing speeds, 43% no significant change and 36% indicated decreasing speeds. As one possible reason for this results they assumed an actual acceleration or deceleration. From our calculations it follows that there may be an apparent acceleration due to the decreasing pitch angle, but the effect is rather small and can be surpassed by other influences easily.

The observational results depicted in Fig. 4 have been obtained by investigating a sample of 40 type III radio bursts. They were recorded by the radiospectralpolarimeter (40–800 MHz) of the Astrophysical Institute Potsdam (Mann et al. 1992). The radial velocity v_r is related to the drift rates D_f measured at the frequency f through:

$$D_f = \frac{f}{2}\frac{1}{N}\frac{dN}{dr}v, \tag{14}$$

assuming emission at the local plasma frequency f_P. We have determined the radial velocities by means of the density model by Mann et al. 1999. Since we have considered the drift of the burst onset only, it is justified to assume emission at the fundamental of the plasma frequency (see Dulk et al. 1984 and Dulk et al. 1987). All bursts where observed during one electron event (date: 1994 December 27 start about 1042 UT) to make sure similar conditions in the solar corona. Fig. 4 shows the distribution of the number of bursts with a certain velocity in the frequency range between 170 MHz and 100 MHz (top) and in the frequency range from 300 MHz to 200 MHz (bottom).

It is obvious that the mean speed of the bursts shifts to higher values in the range of higher altitudes. In the range between 300 MHz and 200 MHz we have found an average velocity of 39 000 km/s and in the lower frequency range an average of 48 000 km/s. Against this, the results of our calculations show that the radial velocity component decreases at low altitudes (at least up to 1.5 $R_{\odot}$) for all initial velocities. But we have not yet considered the influence of the initial pitch angle (up to now an initial pitch angle of $\theta = 0$ has been assumed). The radial

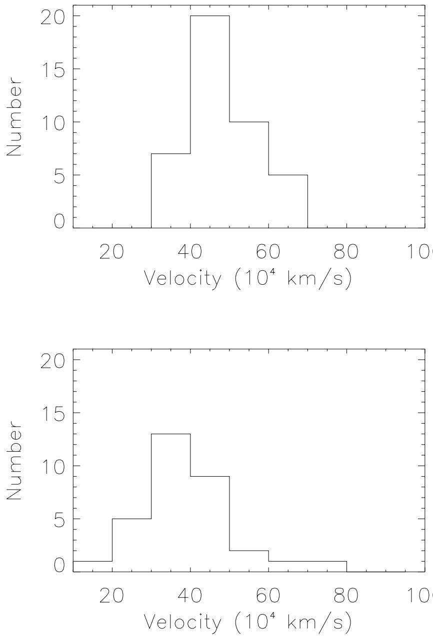

Fig. 4. Histograms of electron speeds deduced from type III bursts on December 27, 1994 in the range of (170–100) MHz (*top*) and (300–200) MHz (*bottom*) (observed at Observatory of Solar Radio Astronomy in Tremsdorf, Germany).

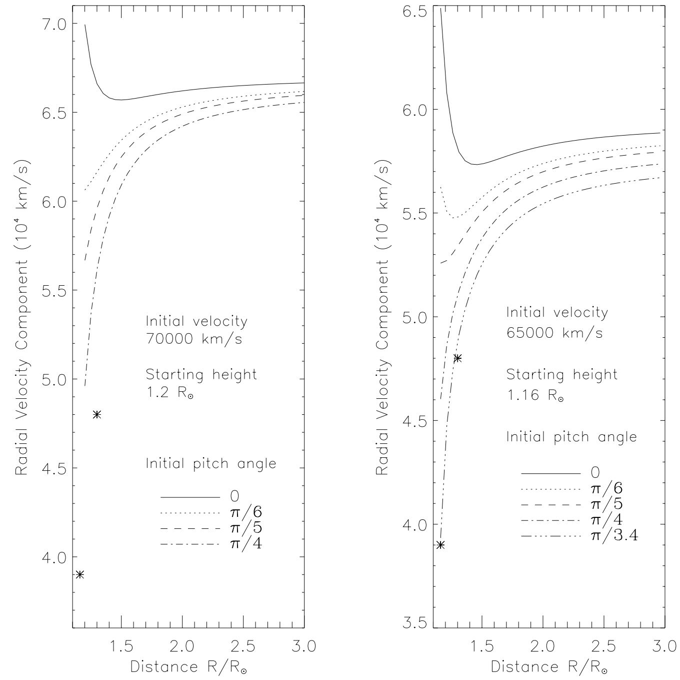

Fig. 5. Radial velocity component as a function of distance from the Sun for different initial pitch angles.

velocity component for different initial pitch angles is depicted in Fig. 5. For the left figure an initial velocity of 70 000 km/s and a starting height of 1.2 $R_\odot$ and the figure on the right an initial velocity of 65 000 km/s and a starting height of 1.16 $R_\odot$ have been choosen.

It is evident that for larger initial pitch angles the radial velocity component increases even at low altitudes. The effect becomes more pronounced if a higher initial velocity is assumed.

Dependent on the initial velocity and starting height the radial velocity can decrease or increase at low distances for the same value of the initial pitch angle (e.g. $\theta = \pi/6$ in Fig. 5). This reveals a variety of possible type III signatures even if Coulomb collisions and the large scale magnetic field are considered only. The average velocities of Fig. 4 are depicted by stars in Fig. 5. A very good fit could be achieved for an initial velocity of 65 000 km/s and an initial pitch angle of 53°. But it has to be emphasized that the last conclusion is related to the special event that we have considered in this work.

The influence of the Coulomb collisions and the large scale interplanetary magnetic field on the observed radiation signature of electron beams depicted in a frequency time spectrum (type III radio burst) is shown in Fig. 6. The curves for a free streaming evolution, i.e. propagation without any interaction with the ambient plasma, are shown in comparison. We have depicted the trajectories for two different velocities, since an electron beam consists of a system of particles with a velocity distribution. Due to the velocity distribution, an electron beam is stretched in the space coordinate with x=vt. From Fig. 6 it can be seen that the spectrum shows a considerable spread in time at a certain frequency compared to free streaming electrons. This spread is caused by the energy loss of the electrons at low coronal heights.

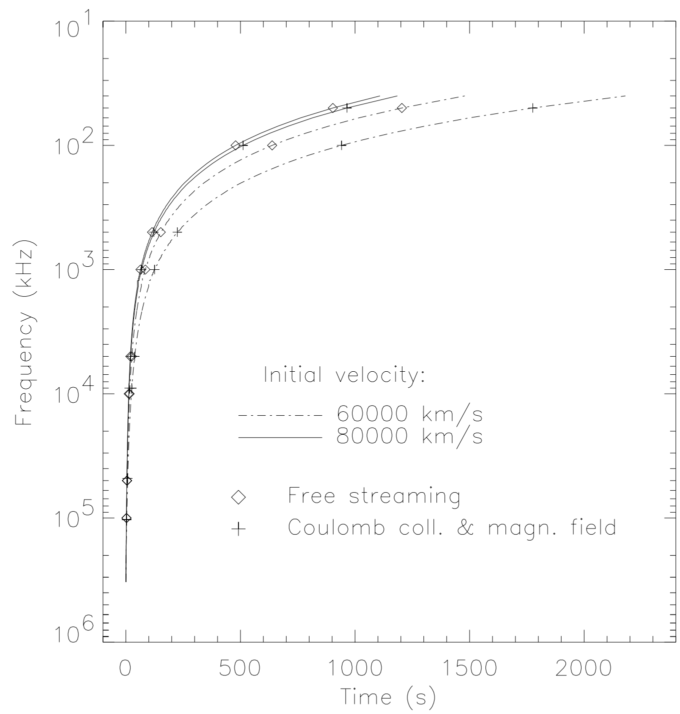

Fig. 6. Frequency-time-spectrum. Comparison of a signature calculated with constant kinetic energy and a signature deduced from the radial energy component in consideration of Coulomb collisions and the large scale magnetic field for two different velocities. The starting height is 1.1 $R_\odot$ and the initial pitch angle zero.

The path length of electrons is also influenced by other interaction processes. Especially the problem of quasi-linear plasma wave generation and the scattering in wave turbulence zones play an important role (see the reviews of Muschietti (1990) and Karlický (1997) where detailed references are given). Further work is necessary for a basic understanding of the beam plasma interaction process and the role of various plasma parameters.

Acknowledgements. This work was supported by DLR under grant no. 50 QL 9602 1.

References

Bai T., 1982, ApJ 259, 341

Bastain T.S., Benz A.O., Gary D.E., 1998, ARA&A 36, 131

Benz A.O., 1993, Plasma Astrophysics: Kinetic Processes in Solar and Stellar Coronae. Kluwer Acad. Publ., Dordrecht

Brown J.C., 1972, Solar Phys. 26, 441

Dulk G.A., McLean D.J., 1978, Solar Phys. 57, 279

Dulk G.A., Steinberg J.L., Hoang S., 1984, A&A 141, 30

Dulk G.A., Steinberg J.L., Hoang S., Goldman M.V., 1987, A&A 173, 366

Emslie A.G., 1978, ApJ 224, 241

Jackson J.D., 1962, Classical Electrodynamics. John Wiley and Sons, New York, p. 429–434

Karlický M., 1997, Space Sci. Rev. 81, 143

Krall N.A., Trivelpiece A. W., 1973, Principles of Plasma Physics. McGraw-Hill, New York, p. 621–624

Leach J., Petrosian V., 1981, ApJ 251, 781

Lin R.P., Larson D., McFadden J., et al., 1996, Geophys. Res. Letters 23, 1211

Lu E.T., Petrosian V., 1988, ApJ 327, 405

Mann G., Auraß H., Voigt W., Paschke J., 1992, ESA-Journal SP-348, 129

Mann G., Jansen F., MacDowall R.J., Kaiser M., Stone R.G., 1999, A&A in press

Mariani F., Neubauer F.M., 1990, In: Schwenn R., Marsch E. (eds.) Physics of the Inner Heliosphere I: Large-Scale Phenomena. Springer Verlag, Berlin Heidelberg, p. 183–204

Melrose D.B., 1985, In: McLean D.J., Labrum N.R. (eds.) Solar Radiophysics. Cambridge University Press, Cambridge, p. 177

Muschietti L., 1990, Solar Phys. 130, 201

Newkirk G.A., 1961, ApJ 133, 983

Schwenn R., 1990, In: Schwenn R., Marsch E. (eds.) Physics of the Inner Heliosphere I: Large-Scale Phenomena. Springer Verlag, Berlin Heidelberg, p. 99

Suzuki S., Dulk G.A., 1985, In: McLean D.J., Labrum N.R. (eds.) Solar Radiophysics. Cambridge University Press, Cambridge, p. 289

Trubnikov B.A., 1965, Rev. Plasma Phys. 1, p. 105–115